Journal of Computer-Aided Molecular Design, **14:** 355–368, 2000.
KLUWER/ESCOM

Research on anti-HIV-1 agents. Investigation on the CD4-Suradista binding mode through docking experiments

Fabrizio Manetti[a], Federico Corelli[a,b,*], Nicola Mongelli[c,*], Andrea Lombardi Borgia[c] & Maurizio Botta[a,b,*]

[a]*Dipartimento Farmaco Chimico Tecnologico, Università degli Studi di Siena, Via A. Moro s.n.c., I-53100 Siena, Italy;* [b]*Centro Interdipartimentale per lo Studio di Sistemi Biomolecolari, Università degli Studi di Siena, Via A. Moro s.n.c., I-53100 Siena, Italy;* [c]*Pharmacia & Upjohn, Viale Pasteur 10, I-20014 Nerviano, Milano, Italy*

Received 7 April 1999; Accepted 3 November 1999

Key words: anti-HIV-1 agents, binding mode, CD4, molecular docking, Suradista compounds

Summary

Sulfonated distamycin (Suradista) derivatives exhibit anti-HIV-1 activity by inhibiting the binding of the viral envelope glycoprotein gp120 to its receptor (CD4). With the aim to propose a possible binding mode between Suradistas and the CD4 macromolecule, molecular docking experiments, followed by energy minimization of the complexes thus obtained, were performed. Computational results show that ligand binding at the CD4 surface involves two or three positively charged regions of the macromolecule, in agreement with the results of X-ray crystallographic analysis of a ternary complex (CD4/gp120/neutralizing antibody) recently reported in the literature. Our findings account well for the structure–activity relationship found for Suradista compounds.

Introduction

Virus infection is initiated by the attachment of a viral particle to a specific receptor on the plasma membrane of the target cell. One of the most striking findings in this field of research is the extraordinary diversity of cell-surface molecules that have been selected by viruses to gain entry into host cells. These receptors include a broad range of glycoproteins with various cellular functions, and also some glycosphingolipids. The identification of viral receptors is of fundamental importance for the development of antiviral drugs that are able to block the infection process before virus entry.

One important feature of viral receptor function is that the so-called 'receptor' may not be sufficient by itself for allowing virus entry into the host cell. In the case of CD4, it has recently become evident that one or several cellular accessory factors are needed for the post-binding events leading to the fusion between HIV-1 and the surface of the target cell [1].

In addition, it is now evident that some viruses are able to use more than one cellular receptor. For example, the surface-envelope glycoprotein gp120 of HIV-1 recognizes both the CD4 glycoprotein and the glycosphingolipid galactosylceramide in two different regions.

Two of the most relevant aspects of HIV infection that have been intensely studied are: (1) the way in which HIV is transmitted and the mechanisms of viral pathogenesis; (2) how can we prevent or reduce transmission and render HIV less pathogenic to the host [2–4].

HIV transmission and pathogenesis are very closely related to the viral envelope glycoproteins. In the CD4-dependent pathway of entry, virus binding takes place at the cell surface and is the result of a highly specific interaction between the principal HIV cellular receptor (the CD4 molecule) and the surface envelope viral glycoprotein gp120 [5]. Subsequently, the fusion between the viral envelope and

*To whom correspondence should be addressed. E-mail: Corelli@unisi.it, Botta@unisi.it, nicola.mongelli@eu.pnu.com

cell membranes allows the virus core to penetrate the cell cytoplasm. Human CD4 consists of an extracellular portion (residues 1–371), a transmembrane segment (372–395) and a cytoplasmic tail (393–433). The gp120 binding site on CD4 is localized on its N-terminal domain (D1), whose structure was recently determined by X-ray crystallographic analysis [6, 7] in the form of D1D2, a soluble two-domain fragment of CD4. Domain D1 resembles very closely the variable domain of an immunoglobulin light chain and has two β sheets, with strands conventionally labelled ABCC′C″DEFG. Strands ABED form one sheet, strands GFCC′C″ the other.

Extensive mutagenesis of the N-terminal domain of CD4 has been carried out to define the residues involved in the interaction. Mutations that influence gp120 binding cluster near the edge of domain 1, which contains strand C″, and the high-affinity binding site for gp120 has been clearly demonstrated to lie between positions 38 and 59; their side chains decorate the C″ edge, forming a ridge about 25 Å long and 12 Å wide, including an exposed phenylalanine at position 43 in the C′C″ turn. Phe^{43} is the dominant determinant and, for retention of high gp120 binding affinity, Arg^{59} can only be replaced by lysine, indicating that an interaction with a basic positively charged amino acid may be necessary at this site [8,9]. Definition of the contact surface on CD4 by mutagenesis is still incomplete, but it is likely to require a region of interaction on gp120 at least 25 Å long and 12 Å wide; in addition, a second region of CD4 domain 1 may supply additional binding energy [10], and finally, it is possible that the gp120 site is a groove rather than a flat surface. These data highlight that the interaction between gp120 and CD4 has been extensively studied because of its potential as a target for specific therapeutic intervention in viral replication [11–13].

A group of compounds structurally related to the non-toxic minor groove DNA binder distamycin (Figure 1 and Table 1), synthesized by Pharmacia & Upjohn, have been extensively studied for their anti-HIV activity [14–17] and proved to be potential candidates for clinical trials [18]. Several were highly potent inhibitors of HIV virus-induced cell killing and viral replication of a wide variety of laboratory isolates.

All these compounds (generally called ‘Suradistas’) contain the amido-N-methylpyrrolenaphthalenesulfonic acid group, but differ in the number of N-methylpyrrole groups as well as in the number and position of sulfonic acids on the naphthalene rings. Structure–function analysis suggests that the number of N-methylpyrrole groups plays a significant role in determining the inhibitory properties of these compounds, since the distance between the naphthalene ring and the ureido function affects the observed anti-HIV activity. Whether this is due to a difference in spacing of the naphthalene moieties or is a direct function of the N-methylpyrrole group has yet to be determined.

The biological activity is also dependent upon the substitution pattern of the naphthalene rings, the 7-aminonaphthyl derivatives being generally more active than the 8-aminonaphthyl analogues. Moreover, in the 7-aminonaphthyl series the number of sulfonate groups, rather than their relative position on the naphthalene ring, markedly affects the antiviral potency, whereas this trend is completely reversed in the 8-aminonaphthyl derivatives. Only compounds **1** and **2**, provided with two naphthylsulfonate moieties, exhibit antiviral activity, although monofunctional derivatives **5**–**8** display RT-inhibiting properties in vitro. Finally, the symmetrically substituted triazine derivative **1a** is more active than its unsymmetrical counterpart **1b** and by far the most potent among all the studied compounds.

The detailed mechanism of action of these derivatives remains to be elucidated. However, due to their polar nature, these compounds are unlikely to enter cells, and their activity has been attributed to the inhibition of viral binding [18]. In fact, several reports have indicated polyanionic compounds as a general class of antiviral agents acting at least in part by interfering at the viral adsorption stage of infection [19, 20]. In particular, various sulfated polysaccharides such as dextran sulfate, sulfated polyesters [21], polyvinyl- and polystyrenesulfonates, and polysulfonated azo dyes (Evans Blue, Direct Blue) have all been reported to interfere with CD4-gp120 binding. Moreover, several organic compounds [22–24], including a series of naphthalene sulfonates, have been shown to suppress HIV-1 infection by disrupting the gp120-CD4 binding interactions.

In order to clarify the mechanism of antiviral activity and identify the step(s) of HIV replication that is affected, the Suradistas were evaluated in a multiplicity of infection acute phase time-of-addition assay as previously described by Cushman [25]. Compound **2b** prevented intracellular HIV-1 proviral DNA synthesis when added during the attachment period of virus with cells indicating that binding of virions was inhibited. Moreover, the same compound appeared to inhibit the fusion process, as indicated by the preven-

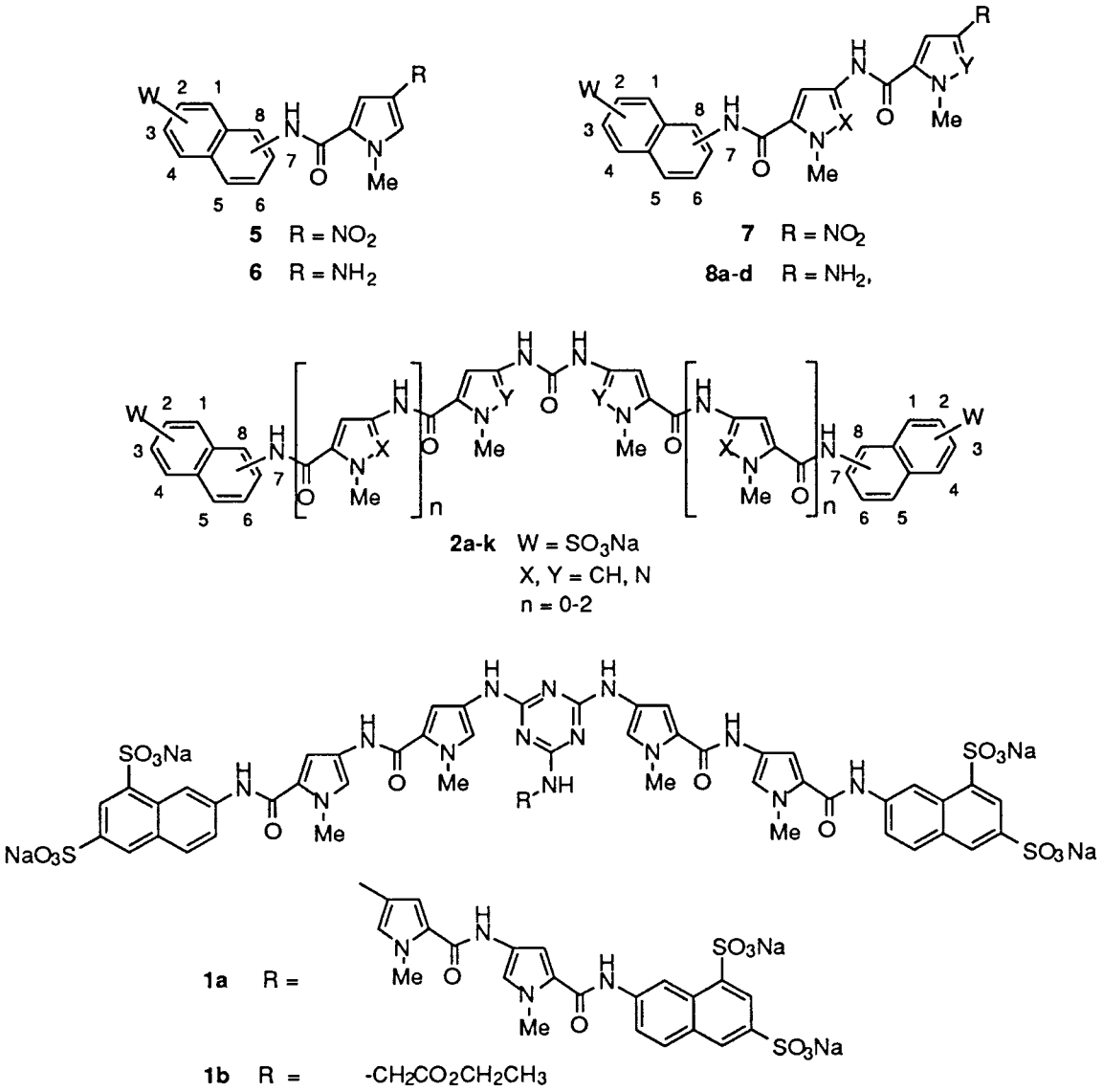

Figure 1. Structure of compounds **1**, **2**, **5**–**8**.

tion of proviral DNA synthesis when compound **2b** was added after viral attachment had already occurred. Waiting a half hour or longer to add any of the compounds failed to inhibit DNA synthesis. On the other hand, ddC (a nucleoside inhibitor of reverse transcriptase) prevented DNA synthesis when added as late as 2 h after virus binding, as reverse transcription was not completed until approximately 4 h. This pattern of inhibition by an RT inhibitor was distinct from that of the ureido-based compounds. In summary, time course experiments previously published by our group [18] clearly demonstrated that inhibition occurred at the surface of the cell and compound **2b** was shown to interfere with attachment of virus to cells, most likely due to an effect on CD4-gp120 interactions, as well as inhibiting the fusion process between virus and cell.

Materials and methods

Calculations and graphics manipulations were performed on Silicon Graphics Indy and O2 workstations. The images shown in Figures 2–5 were prepared using the program InsightII [26]. Starting geometries of all the ligands were generated and energy-minimized

Table 1. Chemical data and anti-HIV activities of compounds **1**, **2** and **5**–**8**

Compd	NH pos.	*X*	*Y*	*W*	*n*	EC_{50} (μM)[a]	IC_{50} (μM)[b]
1a	–	–	–	–	–	0.06	> 200
1b	–	–	–	–	–	3.9	> 200
2a	7	CH	CH	1,3-SO_3Na	1	29.6	> 200
2b	7	CH	CH	1,3,5-SO_3Na	1	4.6	> 200
2c	7	CH	CH	1,3-SO_3Na	2	1.0	86
2d	8	CH	CH	1,3,5-SO_3Na	1	31.6	> 200
2e	7	CH	CH	1,3-SO_3Na	0	80.7	> 200
2f	8	CH	CH	3,5-SO_3Na	1	12.3	> 200
2g	7	CH	CH	4,8-SO_3Na	1	23	153
2h	7	N	N	1,3-SO_3Na	1	7.5	> 200
2i	8	CH	CH	1,5-SO_3Na	1	> 200	> 200
2j	7	CH	N	1,3-SO_3Na	1	7.9	> 200
2k	7	N	CH	1,3-SO_3Na	1	6.5	> 200
5	8	–	–	3,5-SO_3Na	–	> 200	> 500
6	8	–	–	3,5-SO_3Na	–	> 200	> 300
7	7	CH	CH	1,3,5-SO_3Na	–	256	> 200
8a	7	CH	CH	1,3,5-SO_3Na	–	155.7	> 200
8b	8	CH	CH	3,5-SO_3Na	–	34.9	313
8c	7	N	CH	1,3-SO_3Na	–	19.5	> 200
8d	7	CH	N	1,3-SO_3Na	–	> 200	> 200

[a,b] All compounds were evaluated from a high test concentration of 200 μM for their 50% effective antiviral concentration, EC_{50} (reported as the concentration of drug required to inhibit 50% of virus induced cell killing), and their concentration that caused 50% cell death, IC_{50} (reported as the concentration of drug required to reduce cell viability by 50%), utilizing the XTT cytoprotection assay for each congener.

using the program MacroModel-BatchMin [27, 28] equipped with the AMBER* force field [29].

Conformational analysis

Compounds **1** and **2** were subjected to a statistical conformational search with the Monte Carlo Multiple Minimum (MCMM) method, previously described in our publications. The charges for Suradistas were determined according to the procedure defined by Merz for aryl sulfonate derivatives [30]. The GB/SA solvation method, considering water as the solvent, was used. The program BatchMin uses a continuum approach to represent solvent, unlike other programs which use a large number of explicit solvent molecules. Structures are considered the same unless the least squares superimposition of the compared atoms finds one or more pairs of equivalent atoms separated by more than 0.25 Å. Structures were minimized using the Polak-Ribière Conjugate Gradient method until the derivative convergence was 0.001 kcal/mol Å. Every structure which is more than 6 kcal/mol above the minimum-energy conformation was rejected and the search was continued until each conformer in this energy range was located at least three times.

Atomic coordinates for the structure representing the N-terminal fragment of CD4 were obtained from the Brookhaven Protein Data Bank (code 2cd4). All water molecules were removed and excluded from the calculations; hydrogen atoms were added in their idealized positions.

Molecular docking

The program MacroModel provides a useful tool for interactively identifying possible binding interactions between a pair of molecules, one of which is called the ligand (compounds **1** and **2**) and the other the site (the protein). The energies of interaction are based on steric contributions from the AMBER* all-atom force field and electrostatic contributions from any atomic charges present (computing according to data in the force field file). During the docking operation, the ligand molecule can be moved freely relative to the site. The current configuration can be minimized at any time, with any combination of ligand or site held rigid.

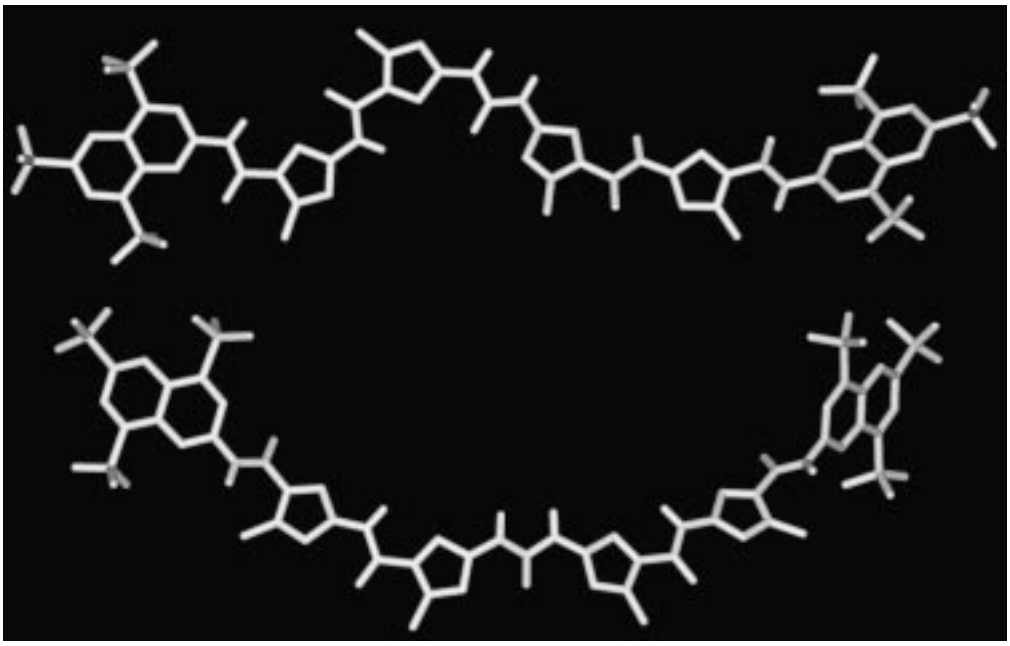

Figure 2. Upper: minimum energy conformation of ligand **2b**. Lower: low energy conformation (2 kcal/mol over the global minimum) of **2b** used as putative bioactive conformation throughout this work.

In our case, the molecule whose internal geometry was kept rigid was the site.

Complexes between CD4 and ligands **2** were built in the following manner. One of the preferred conformers of each compound, showing a symmetrical shape with respect to the ureido carbonyl group, was interactively docked into the C′C″D strands of the CD4 molecule so that pi-stacking involving the naphthyl ring of the ligand and the aromatic side chain of Phe^{43} was created. In addition, the basic side chain of an exposed arginine at position 59 (which lies in the sequence between the C and D strands) contracts some salt-bridges with the sulfonate group at the 3-position of the ligand. Unfavourable contacts were removed using the translation-rotation feature.

Starting from CD4-**2** complexes, the ureido moiety of the ligands was opportunely modified and a third side chain was added to build the complexes between CD4 and compounds **1**.

Optimization of the CD4-ligand complexes

The resultant complexes were then optimized through an automatic, interactive procedure which minimizes both steric and electrostatic interactions until the energy gradient RMS was 0.05 kcal/mol Å. The low energy complexes were subjected to further optimization using a combined energy minimization and conformational search protocol that we had used previously in calculation of substrate-serine protease complexes. On the docked bimolecular complexes, the MCMM conformational search algorithm of BatchMin was used with 2–7 randomly selected degrees of freedom of the ligand varied at each Monte Carlo step, involving translation and/or rotation of the substrate molecule. The geometry of the binding site was kept rigid. A *trans* conformation for all the amide bonds of the ligand was assumed on the basis of data previously reported by our and other groups [17, 31]. Suradistas are able to rotate and translate with respect to the amino acid residues of CD4, thus possessing six degrees of translational/rotational freedom. Conformational flexibility is taken into account by rotating around single bonds of the ligand, thus generating complexes with different conformers of the ligand. At each step, a new configuration is generated by making random changes to each variable (the rotatable bonds, x/y/z translations, and x/y/z rotations). The energy of the new configuration is calculated and accepted or rejected according to user-defined criteria. This protocol has been used to sample a large part of the energy hypersurface and look for other possible binding geometries.

Because of the large number of atoms in the model, to correctly optimize the complexes of **1** and **2** with CD4, the following constraints had to be imposed:

(a) A subset, centered on the ligand, comprising only the inhibitor and a shell of residues surrounding the hypothetical binding site of CD4, and within 12 Å of the ligand was created and subjected to energy minimization. While compounds **2** interact with amino acid residues within the C′C″D strands, in the case of CD4-**1** complexes, a considerable number of binding-site residues were included in the energy minimization (including all the CD4 residues reported in contact with gp120 and ranging from 25 to 64) [38], due to structural features of these ligands (i.e. three amido-N-methylpyrrolenaphthalene sulfonic acid side chains). The inhibitor and all amino acid side chains of the shell were unconstrained during energy minimization to allow for reorientation and thus proper hydrogen-bonding geometries and van der Waals contacts.

(b) All the atoms external to the subset remained fixed, even if their non-bonded interactions with all the relaxing atoms had been calculated.

The default non-bonded cutoff protocol employed by the BatchMin program was modified. Thus, a van der Waals cutoff of 12.0 Å, an electrostatic cutoff of 20 Å, and a hydrogen bonding cutoff of 4 Å were utilized for all calculations.

Energy minimization of the complexes was performed using the Polak-Ribière Conjugate Gradient procedure, and terminated either after 10,000 iterations or when the RMS gradient fell below 0.01 kcal/mol Å. The GB/SA solvation model (solvent water) and a constant dielectric constant of 1.0 were used during minimization employing the AMBER* all-atom force field.

GRID calculations

Using the GRIN program, the CD4 coordinates were converted to an input structure for the GRID program. GRIN checks the input structure for errors and assigns to each atom appropriate parameters necessary for the GRID calculation.

GRID (version 16) [32, 33] places a three-dimensional grid around the protein and calculates for each grid point the energy of interaction (containing contributions from the van der Waals, electrostatic, and hydrogen bond interactions) between the probe and all the protein atoms. The probe used was O= (an oxygen bonded to only one atom, e.g., to the sulfur of sulfonate groups) and C1= (aromatic sp2 carbon atom bonded to one hydrogen atom). The program GROUP was also used to find possible interaction sites for a small molecule (called the Probe Molecule) with CD4. GROUP requires the structures of both CD4 and the Probe Molecule and a set of maps (corresponding to each polar atom present in the probe) previously calculated by GRID. The program begins by placing one of the polar atoms of the probe at a position on the corresponding GRID map which allows for favourable interactions with CD4. Similar searches are performed for a second and a third polar atom of the probe. Each new position would have to be at the appropriate distance from the first one to give a possible binding mode of the Probe Molecule on CD4. Non-polar atoms of the probe are all used for the evaluation of steric clashes and, thus, for final fitting of Probe Molecule to CD4. Finally, all the possible positions for the Probe Molecule are stored for graphical display and/or further analysis.

Results

In an effort to rationalize biological data of compounds **1**, **2**, **5**–**8**, we resorted to molecular modeling in an attempt to gain an insight into both the possible biologically active conformation(s) of these ligands and their mode of interaction with CD4 or gp120. Investigation of a possible model of interaction between these ligands and viral envelope glycoproteins (particularly gp120) was not considered at this stage because all compounds failed to directly inactivate infectious virions [18]. In contrast, the ligands clearly possess the appropriate chemical functionalities that allow to establish either ionic or hydrogen bonding interactions with CD4, which is rich in basic amino acid residues (the surface of D1D2 has many positively charged amino acids and the calculated pI of residues 1–183 is 10.0) [7].

However, no information to date has addressed the issue of how such compounds can selectively and productively dock into the target. To begin to broach this issue, we performed docking experiments using the program MacroModel with the goal to produce a complex between ligand and CD4 that optimizes geometric and chemical complementarity. For this purpose, we used the three-dimensional structure of an N-terminal fragment of CD4 determined by X-ray crystallography and refined at 2.4 Å resolution [6] (Brookhaven Protein Data Bank code 2cd4).

Since many of the residues implicated in the binding of HIV-gp120 span from positions 38 to 52 involving CD4 C′ and C″ strands, we focused our at-

Table 2. Overview of hydrogen bonds shown by Suradistas docked to CD4. Every compound is represented by its energetically best result

Compd	Subsite 1		Subsite 2		Subsite 3		Other locations[a]	
	Hs	Hm	Hs	Hm	Hs	Hm	Hs	Hm
1a	3Arg^{59,b} 1Ser^{42}	1Leu^{44}	2Lys^{50}	1Lys^{50}	2Gln^{33} 2Lys^{35} 2Lys^{29} 2Lys^{90}	1Glu^{87,a}	1Phe^{26} 1Gly^{47}	
1b	3Arg^{59} 1Ser^{42}	1Leu^{44}	2Lys^{50}	1Lys^{50}	–		1Lys^{35} 1Gly^{47}	
2a	3Arg^{59} 1Ser^{42}		1Lys^{50}	2Lys^{50,a}	–			1Gln^{40}
2b	1Arg^{59} 2Ser^{42}	1Phe^{43} 1Ser^{42}	2Asn^{30} 2Asn^{32} 2Lys^{50}	1Lys^{50,a}	–			1Gln^{40}
2c	3Arg^{59} 1Ser^{42}		2Lys^{50} 1Ser^{79}		–			2Gln^{40}
2d	2Arg^{59} 1Ser^{42}	1Ser^{42,a}	2Lys^{50}	1Lys^{50}	–			1Gln^{40}
2f	3Arg^{59} 1Ser^{42}		2Lys^{50}	1Lys^{50}	–			1Gln^{40} 1Pro^{48}
2g	2Arg^{59} 1Ser^{42}	1Ser^{42,a}	2Lys^{50} 1Asn^{30}	1Lys^{50,a}	–			1Gln^{40}
2i	2Arg^{59} 1Ser^{42}		1Ser^{49}		–			1Gln^{40}

[a] Residues interacting with Suradistas backbone.
[b] Number of interactions and amino acid residue involved. Hs: H-bonds with side chain; Hm: H-bonds with main chain.

tention on that region of the protein as possible ligand attachment site.

Conformational analysis

Building and optimization of compounds and conformational analysis protocols were reported in our previous publications [16, 17, 34]. The conformational search was performed using a continuum water solvation model as implemented in BatchMin. As a result, compound **2b** (taken as a representative of the whole class of compounds **2**) assumes, at the lower energy level, an extended conformation which assures the maximum distance between the sulfonate groups, while the shape of the whole molecule is quasi-helicoidal with the N-methyl groups describing a complete turn. In addition, one of the preferred conformations of **2b**, among the about 10,000 structures generated by this program, appears as a highly symmetrical, quasi-planar arc of circumference, as expected on the basis of the symmetrical pattern of its NMR spectrum [16] (Figure 2). The planar structure of the ligand is in good agreement with the extensive delocalized system formed by the ureido moiety, the pyrrole rings, the adjoining amide groups and the naphthalene rings. The calculated energy associated with the symmetrical structure was 2 kcal/mol over the minimum energy conformation.

Interestingly, in this conformer the distance between the sulfonate groups at the 3-position of the two naphthalene units is 24–26 Å, which is in full agreement with the 25 Å extension of the ridge containing the C″ strand [6]. These observations highlight a possible good shape complementarity between conformations of the ligands and the ridge on the CD4 macromolecule, leading us to choose the symmetrical, planar structure as the putative bioactive conformation of compound **2b**.

Building procedure of structural models

Complexes between CD4 and ligands **1** and **2** were obtained applying the following procedure. Since the most important functional group of the ligand respon-

sible for a possible binding to CD4 should be the sulfonate group, one of the naphthalene sulfonate moieties was positioned so that some salt bridges between sulfonate groups of the ligands and the basic group of the Arg^{59} side chain projecting toward the C′C″ corner were created. In addition, pi-interactions between the aromatic ring of the ligands and the side chain of Phe^{43} were formed. The orientation of the pyrrole spacers and the second naphthalene ring of the ligands on the surface of the macromolecule was settled so as to optimize the shape complementarity between the preferred conformation of the ligands and the C′C″D strands. The resultant complexes were then optimized using a combined energy minimization and conformational search protocol [17, 35].

Receptor ligand interactions

When compound **2b** in its symmetrical conformation was docked into the X-ray structure of CD4 (Figure 3), very good interactions between the naphthalene sulfonate groups of the ligand and two distinct regions (hereafter referred to as subsite 1 and subsite 2, respectively) on the CD4 surface were found (Table 2). Particularly, an extended network of hydrogen bonds involving Ser^{42} (from the C′C″ corner) and Arg^{59} side chains was found within subsite 1. Moreover, pi-interactions between the phenyl ring of Phe^{43} of CD4 and the naphthyl moiety of the substrate play a fundamental role in stabilizing the CD4-**2b** complex. The planes of the two aromatic rings define a dihedral angle of 147 degrees, the centroids of the rings being at a distance of around 3.8 Å.

Asn^{30}, Asn^{32} (both from the CC′ corner), and Lys^{50} (from the C″D corner), surrounding subsite 2, establish hydrogen bonds with sulfonate groups on the other edge of the ligand. Other favourable van der Waals contacts are found between pyrrole spacers of the ligand and Ile^{34} and Pro^{48}. In addition, hydrogen bonds involving Gln^{40} (backbone carbonyl group) and Lys^{50} (backbone NH group) are found. Interestingly, all the amino acid residues involved in the CD4-ligand interactions lie in the sequence 38–59, which is thought to be a fundamental cluster for CD4-gp120 interactions [6, 7].

In order to further test this binding model and obtain an insight into the possible relationship between the structural features of CD4-**1** and -**2** complexes and the biological activity of these compounds, the same computational study was performed starting from the other ligands.

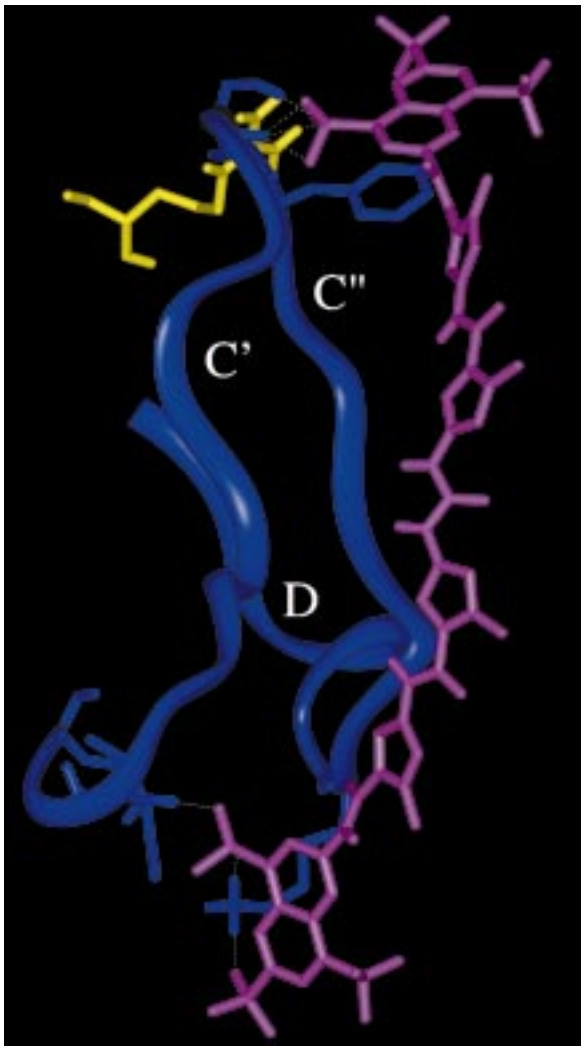

Figure 3. CD4-**2b** complex. Ribbon representation of sequence 30–57 including C′, C″ and D strands of CD4 (in cyan), and ligand **2b** in purple. Side chains of Ser^{42}, Phe^{43}, and (in yellow) Arg^{59} are depicted at the top of the figure. Pi-interactions between the naphthalene ring of the ligand and the Phe^{43} side chain are evident. At the bottom, side chains of Asn^{30}, Asn^{32}, and Lys^{50} are shown. Green dashed lines represent electrostatic interactions (hydrogen bonds and salt bridges) between CD4 amino acids and sulfonic moieties of **2b**. The direction of the view is from the GFCC′C″ face [6].

The complex between compound **2a** and CD4 showed very similar features with respect to the **2b**-CD4 complex. Particularly, hydrogen bonding interactions between the sulfonate group at the 3-position and Arg^{59}, and (on the other side of the ligand) between the sulfonate at the 1-position and Lys^{50} were found.

The distance between the naphthalene ring and the ureido function, as determined by the number of N-

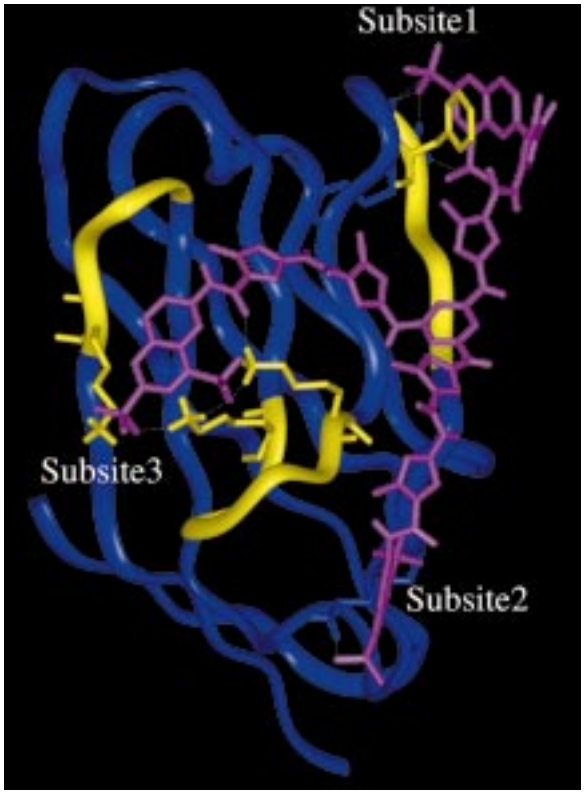

Figure 4. CD4-**1a** complex. Two side chains of compound **1a** (purple), projecting its naphthalene moieties toward the top and the bottom of the figure, are nearly parallel to the C″ strand (yellow, on the right side of the figure). The third side chain of the ligand binds in a large groove whose walls are represented by the FG (yellow, on the left side of the figure) and CC′ (yellow, in the middle of the figure) corners of CD4. The most important amino acid side chains of the three binding sites on CD4 are also shown. The triazine moiety of the ligand overlaps with the C″ strand. Green dashed lines represent hydrogen bonds and salt bridges between CD4 and the ligand. The ribbon diagram is extended to the complete D1 domain of CD4. The direction of the view is from the GFCC′C″ face of CD4 [6].

Figure 5. CD4-**1a** complex. Contacts between ligand **1a** and the hydrophylic region defined by the FG corner (top, yellow) and the CC′ corner (bottom, yellow). The ribbon diagram shows this C-shaped surface and amino acid residues interacting with ligand **1a**. An extended electrostatic network involving some acidic and basic amino acids of CD4 and sulfonate groups of compound **1a** is also evident (green dashed lines).

methylpyrrole spacers, has an effect on the observed anti-HIV activity. In particular, while an increment in activity is observed for **2c** (a compound having the same naphthyl moieties as **2a** but two more spacers in the backbone), a decrease in the activity value is observed in the case of a shorter molecule, such as **2e**.

Examination of the complexes obtained from each of compounds **2a**, **2c** and **2e** quite well accounts for their different biological activity. In fact, compound **2a**, with the sulfonate groups at the 3-position of the two naphthalene moieties at the proper distance of 24–26 Å, fits in an excellent way the C′C″D regions of CD4. A good complementarity is still observed for compound **2c**. In this case, the most favourable interactions are pi-stacking between the aromatic ring of the ligand and the Phe^{43} side chain; moreover, a couple of hydrogen bonds between the Gln^{40} amide side chain and the carbonyl group of an amido-N-methylpyrrole spacer were found. The second naphthalene sulfonate moiety interacts with Lys^{50} and, due to a higher relative distance between the naphthyl moieties, with the Ser^{79} side chain.

Starting from the previously described interaction model (i.e., the naphthyl moiety of ligand **2e** interacting with Arg^{59} and Phe^{43} side chains), it was impossible to dock the second naphthyl group of ligand **2e** on the surface of the macromolecule to obtain a profitable interaction without strong steric repulsion. Attempts to dock compound **2e** in different ways into the C′C″D strands were unsuccessful. These results are in full agreement with biological data showing a higher EC_{50} value for **2e**.

When the position of sulfonate groups on naphthyl moieties is changed, no substantial differences in CD4-ligand interactions were observed. In fact, in the CD4-**2g** complex the two sulfonates at the unusual 4-position establish salt bridges with Arg^{59} and Lys^{50}, respectively, and an additional hydrogen bond involving Asn^{30} was also found. Each of the two sulfonate groups at the 8-position is involved in an intramolecular hydrogen bond with the amide group of the ligand.

The increased activity of pyrazole derivatives **2h**, **2j** and **2k** with respect to **2a** is difficult to rationalize on the basis of the proposed model. A possible explanation could be found in additional hydrogen bonds involving nitrogen atoms of pyrazole rings with some amino acid residues of CD4 (side chain of Gln^{40}). However, further investigations are requested to confirm that additional hydrogen bonds may be sufficient by themselves to account for the differences in the biological activity of these compounds.

The complex between CD4 and compound **2f** shows good van der Waals contacts with Gln^{40}, Gln^{41} and Phe^{43}. Hydrogen bonds between Arg^{59} and Ser^{42} side chains with the sulfonate group at the 5-position, as well as between Gln^{40} and the ligand amide group, were found. The other arm of the ligand interacts with Ile^{34}, Pro^{48}, Ser^{49} and Lys^{50}: in particular, the ligand amide and the sulfonate group at the 3-position establish hydrogen bonds with Pro^{48} and Lys^{50} (both terminal and backbone NH groups), respectively.

Very similar contacts can be highlighted in the case of the CD4-**2d** complex. The most relevant difference is an intramolecular hydrogen bond between the sulfonate group at the 1-position and the amide group of the ligand.

Finally, the lack of a sulfonate group at the 3-position might account for the inactivity of compound **2i**.

In the case of complexes between CD4 and compound **1a** (Figure 4), two of the three side chains of the ligand assume a conformational disposition very similar to that of compounds **2**. In fact, many conformations of **2** showed amido-N-methylpyrrolenaphthalene sulfonic acid chains symmetrically oriented with respect to the ureido moiety; in a similar way, two chains of compound **1a** in the complex with CD4 are in a quasi-symmetrical orientation with respect to the triazine group. Both compounds **1** and **2** are nearly parallel to the C″ strand, while the third side chain of compound **1a** binds in a C-shaped portion of the CD4 surface, very similar to a large groove (Figure 5). Both the CC′ and FG corners (residues 29–35 and 87–90, respectively) as well as short amino acid sequences of the C, C′, F, and G strands constitute the wall and the floor of the groove, respectively. Strands C and C′ are near to the triazine moiety of compound **1a**, while strands F and G are far from it.

The Phe^{43} side chain (Figure 4) undergoes a conformational rearrangement projecting the aromatic ring toward the pyrrole group bound to the naphthyl moiety of the ligand, but, despite this rotation, pi-interactions between naphthalene and the aromatic ring of the Phe^{43} side chain are retained. In addition, the sulfonate group at the 3-position gives rise to salt bridges with the guanidinium moiety of Arg^{59}, while the sulfonate group at the 1-position interacts with the amide NH group of Leu^{44}. Some van der Waals interactions involving Gln^{40} and Gly^{41} were also observed.

The other arm of the ligand molecule establishes hydrogen bonds between sulfonates and both the amide and the ammonium NH of Lys^{50}. Van der Waals contacts involving Pro^{48} and the two pyrrole spacers of this portion of the ligand were also found.

The most significant interactions between CD4 and compound **1a** are contacts between the above described groove and the third side chain bound to the triazine moiety (Figure 5). The ligand fits very well on the CD4 surface by interacting with Gln^{25}, Asp^{88}, Glu^{87}, Glu^{85}, Gln^{33}, His^{27}, Lys^{29}, Lys^{35}, and Lys^{90}, thereby leading to a very stable complex. In particular, the backbone of the ligand interacts by hydrogen bonding with the carbonyl oxygen of Phe^{26}, while the imidazole ring of His^{27} establishes pi-interactions with one of the N-methylpyrrole spacers of the ligand, the planes of the two aromatic rings being nearly parallel and the centroids of the rings lying at a distance of approximately 3.3 Å. The naphthyl ring is directed toward a hydrophylic region of CD4 with some positively charged amino acids (subsite 3), and its sulfonate groups interact electrostatically (hydrogen bonding and salt bridges) with the side chains of Gln^{33}, Lys^{29}, Lys^{35}, and Lys^{90}. Salt bridges between Glu^{85}-Lys^{29}, Glu^{85}-Lys^{35}, and Glu^{92}-Lys^{90} side chains complete the ionic network of this portion of CD4.

The most significant difference between the two complexes CD4-**1a** and CD4-**1b** is due to the lack in **1b** of a third amido-N-methylpyrrolenaphthalene sulfonate side chain and, consequently, of its respective interactions with CD4. However, van der Waals contacts between the ethyl group of the NH-CH_2-COOEt

moiety of **1b** and the methylene portion of the His^{27} side chain, as well as an additional hydrogen bonding interaction between the carbonyl oxygen of the ester and the Lys^{35} side chain, were observed.

Analysis of all CD4-**1** and -**2** complexes showed a good shape complementarity between the ligands and CD4 surface (with the exception of ligand **2e**); in addition, while one of the NH groups of the triazine ring of **1a**,**b** contributes to the binding of these ligands to CD4 by hydrogen bonding to the carbonyl group of Gly^{47}, the ureido moiety in **2** is not able to interact with the CD4 surface, since its hydrogen atoms are oriented toward the CD4 surface in such a way that they cannot afford any binding contribution. In fact, distances between these hydrogens and carbonyl oxygen atoms of Gly^{47} and Lys^{46} are no less than 4.8 Å and 6.7 Å, respectively, thus precluding hydrogen bonding. In contrast, the triazine group of **1** is able in our model to place itself deeper on the CD4 surface than compounds **2**, thereby providing a stronger contribution to binding. This different spatial disposition of the triazine ring with respect to the ureido moiety is due to the flexibility of the $C_{triazine}$-N_{amine} bond, which allows for a dihedral angle of about 40 degrees between the plane of the triazine ring and the plane of the two pyrrole rings bound to it.

Ligands occupying different binding positions

The docking studies and MCMM conformational search have revealed alternative binding modes of Suradista compounds on the CD4 molecular surface, due to the possibility for the ligand to rotate and translate with respect to the amino acid residues of the site. For example, starting from the complex between CD4 and **1a**, two spatially separate orientations of the ligand on the CD4 surface, not involving subsites 1, 2, and 3, were found. In the first alternate binding geometry, the three naphthalene sulfonic moieties of the ligand interact primarily with Lys^{22}, Arg^{58}-Lys^{1}-Lys^{2}, and Lys^{166}-Lys^{167}, respectively. In the second one, the sulfonate groups establish hydrogen bonds with Arg^{58}, Lys^{8}, and Lys^{46}-Lys^{72}, respectively. Although the calculated energy values associated with these complexes are similar, the original complex is slightly favoured (about 5 kcal/mol) over the two alternative binding models.

Other complexes with even higher energy values were also found. For instance, starting from the second alternate model, the ligand can easily evolve in a new conformation lacking the interactions with Lys^{72} and Lys^{46}, and allowing for hydrogen bonding between the naphthalene sulfonic substituent and Arg^{59}. Its complex with CD4 was energetically less favourable by about 7 kcal/mol.

Moreover, on the basis of the rotation around single bonds of the ligands, the computational procedure applied is able to generate a population of complexes differing in the conformational properties of the ligand. In particular, in the case of the CD4-**1a** complex, the distance between the naphthalene moieties ranges between 12 Å and 27 Å, and the maximum value was found in a conformation of the ligand very similar to that described in the original complex.

Although we cannot claim that an exhaustive search was performed on each ligand, the calculations described above have been suggested to be adequate to search the conformational space of inhibitors with approximately 12–14 rotatable bonds docked to a binding site [36]. In addition, although we have used this procedure in such a manner that the rotational and translational degrees of freedom of the ligands are considered, the positional and conformational search complexity was reduced by the presence of the delocalized pi-system extended to the whole molecule of the ligand, which confers an ‘intrinsic’ rigidity to Suradista compounds. Moreover, the overall dimensions of both the CD4 ($65 \times 35 \times 25$ Å) and Suradista molecules should be considered. Since many conformers of compounds **1**–**2** show a sulfonate-sulfonate distance higher than 20 Å, the number of possible orientations of a given ligand on the CD4 surface may be expected to be relatively small.

In the light of these considerations and taking into account GRID results (see below), no further attempt was made to locate additional points for CD4-Suradista interactions.

GRID calculations

In the hope of validating the structural information obtained by docking experiments concerning Suradistas orientations on the CD4 surface, a subsequent molecular modeling study using the program GRID has been carried out. GRID is a program especially developed for calculation of favourable binding sites on macromolecules. The program calculates the intermolecular interaction energy between the macromolecule and a probe around the macromolecule itself. By contouring the interaction energy at various levels, it is possible to locate preferred binding sites for a number of chemical groups.

In this study we have performed a series of GRID calculations in order to determine the most favourable binding sites for probes resembling the different functional groups of the Suradista molecules and, consequently, to determine the orientation of the ligand on the CD4 surface. Sulfonate oxygen and aromatic carbon probes were chosen for GRID runs.

On the basis of the model derived from docking studies, favourable interaction sites for oxygen and aromatics were expected to be found in correspondence to those positions in CD4 where the sulfonate and aromatic (naphthalene, pyrrole, and triazine) groups of the docked ligand lie. GRID calculations using an oxygen atom probe indicated the presence of three preferred binding sites (−11 kcal/mol) close to Lys^{1}-Lys^{2}-Val^{93}-Gln^{94}, Lys^{29}-Lys^{90}-Gln^{33}, and Arg^{58}-Pro^{68}, respectively. While the first two positions were already identified as binding positions in models described for compound **1a** (the first alternate and the original orientation, respectively), the last binding site was never found before during molecular docking simulations. An additional contour map located in the region between Arg^{59} and Phe^{43} was found when contoured at an energy level of −8 kcal/mol.

The aromatic probe at the lower energy level (−4 kcal/mol) predicts five contour maps corresponding to the positions of the three aromatic rings of the third side chain and the triazine moiety of the docked compound **1a**. The remaining map is located within the region close to Arg^{58}, predicted by docking experiments in the two alternate orientations proposed for compound **1a**.

Some additional GRID calculations using as a 'Probe Molecule' the 2-naphthalene sulfonate anion (PM1) and the 6-formamido-2-naphthalene sulfonate anion (PM2), were also performed.

The energetically most relevant orientation of PM1 and the third best orientation of PM2 lie in a region close to the naphthalene sulfonate moiety of the third side chain of compound **1a** (subsite 3 on CD4). The second best orientation of PM2, with the sulfur atom about 3 Å apart from the sulfur atom at the 1-position of the ligand, was found in the same region of space. The second and third energetically most relevant orientations of PM1 were found in the proximity of subsite 2 on CD4. The distance between the sulfur atom of the probe and the sulfur atom at the 1-position of the ligand was calculated to be about 1 Å in both cases.

Differences in the orientation of the Probe Molecules with respect to the corresponding molecular portions of **1a** can be justified taking into account that the orientation of the naphthalene sulfonate groups of the ligand is influenced by the remainder of the molecule.

Discussion

The findings reported above may allow some conclusions to be drawn. In particular, the positioning of the Probe Molecules within two binding sites previously found by docking simulations (subsites 2 and 3) strengthens the opinion that most likely these regions represent or include the 'real' binding site of **1a**. Moreover, subsite 1 could reasonably be considered as a Suradista potential binding site in the light of the following considerations: (i) molecular docking experiments showed the complex between CD4 and compound **1a** interacting with subsites 1, 2, and 3 to be energetically favoured; (ii) hypothetical models recently reported [24, 37] and based on several polyanionic cosalane derivatives led to the conclusion that the two negatively charged carboxylate residues of cosalane may be bound to the two adjacent, positively charged Arg^{58} and Arg^{59} residues of CD4; (iii) experimental evidence indicates that subsite 1 (Arg^{59} and Phe^{43}) is very important for gp120 binding to CD4.

Results from GRID simulations are also in agreement with the binding model proposed for compounds **2**. In fact, the side chains of compounds **1** interacting with subsites 1 and 2 possess conformational properties very similar to compounds **2** (i.e., side chains symmetrically oriented with respect to the central ureido or triazino moieties, quasi-planar structure, and similar distance between sulfonate groups). Moreover, the distance between the sulfonate groups of **1a** interacting with subsites 2 and 3 is by far lower than 25 Å, thus making the binding model involving compounds **2** and subsites 2 and 3 quite unplausible. Analogous considerations could be made about the interaction between compounds **2** and subsites 1 and 3.

Relationships between structural features of compounds **1**-**2** and binding affinity to CD4 can be gathered from the analysis of CD4-ligand complexes. The proposed model is able to rationalize the effect of the distance between the naphthalene rings on the observed activity for compounds **2**. Particularly, compound **2a** seems to be the optimal ligand for CD4, showing the proper distance of 24–26 Å between sul-

fonate groups on the two naphthalene rings. In the case of compound **2c**, due to the higher distance between the naphthalene moieties, additional hydrogen bonds involving the Ser^{79} side chain were observed. This fact suggests that **2c** would be at least as good as **2a** as a CD4 ligand. This idea is in agreement with the experimental evidence. Finally, on the basis of the proposed binding mode, compound **2e** seems to have structural features avoiding a profitable interaction with the CD4 surface.

The results obtained in the present investigation can also explain biological data associated with compounds **1**. **1b** can bind CD4 in the same way as reported for **2a**, and its higher activity may be attributed to further interactions of the triazine ring and ester side chain with CD4 amino acids. The marked increase in the activity of **1a** can be explained taking into consideration the interaction of the third naphthylsulfonate moiety with a third accessory binding site (subsite 3).

In the light of the biological and computational results reported above, we infer that compounds **1**,**2** might interact with CD4 by the attachment of their naphthylsulfonic moieties to three different hypothetical binding sites surrounding Phe^{43}-Arg^{59}, Lys^{29}-Lys^{35}-Lys^{90} and Lys^{50}, respectively. In spite of the lack of activity of ligands **5**–**8** possessing only one naphthylsulfonic moiety, to justify the biological data of compounds **8b** and **8c** we cannot exclude a model of interaction which implies monodentate binding of these ligands to the CD4 surface, though we are not able to identify the most probable binding site.

Very recently, after the completion of this work, the structure of an HIV gp120 envelope glycoprotein complexed with the CD4 receptor and a neutralizing human antibody (ternary complex) has been reported in the literature [38]. The ternary structure was solved by X-ray crystallography at 2.5 Å resolution and shows that residues of CD4 in contact with gp120 are concentrated in the span from 25 to 64 with Phe^{43} and Arg^{59} of CD4 establishing multiple contacts. In particular, 63% of all interatomic contacts involve the span 40–48 in the C′C″ strands of CD4, and Phe^{43} accounts on its own for 23% of the total. Moreover, three CD4 lysine residues are implicated in binding (residues 29, 35 and 46).

Accordingly, the amino acids of CD4 involved in the CD4-Suradista and ternary complexes are basically the same. Both the experimentally and computationally obtained complexes agree in highlighting the fundamental role played by Phe^{43} in interacting with compounds **1**,**2** and gp120 sequences, respectively. While in CD4-**1** and -**2** complexes Phe^{43} determines the basic orientation of the ligands on the CD4 surface, so that these compounds interact with the C″ ridge present on CD4, in the ternary complex the phenyl ring of Phe^{43} is the only non-gp120 residue contacting the so-called 'Phe^{43} cavity' on gp120, forming a lid that covers the bottom of this cavity. Moreover, the guanidinium moiety of Arg^{59} is very important in stabilizing both complexes (CD4-Suradista and the ternary one) by salt bridges with acidic groups (sulfonate and carboxylate, respectively). In addition, two of the three CD4 lysine residues interacting with gp120 in the ternary complex are also involved in stabilizing the CD4-**1a** complex (i.e., residues 29 and 35).

In principle, a set of conformers obtained from a Monte Carlo search could be analyzed further by methods that adequately take solvation and entropic effects into account for a final comparison of the bound conformers and eventually a comparison of relative binding affinity among different ligands [36]. However, the simple methods described thus far in the literature have been mainly applied to the study of ligands which are neutral and approximately the same size. Moreover, these models neglect some factors which are key to binding, such as, for instance, the solvation/desolvation of the ligand and the macromolecule [39], which may deeply influence the binding process when ionic ligands such as Suradistas are involved in the interaction. On the other hand, quantitative prediction of the affinity of a ligand for its receptor (e.g. via free-energy perturbation calculations) can be costly and time-consuming. In the light of these considerations, no attempt has been made at this stage to obtain a quantitative correlation between binding energy and biological activity for our ligands.

Conclusions

The binding model described above can explain the activity of Suradista compounds in terms of their attachment to the surface of CD4, which in turn prevents the interaction of CD4 with the viral envelope glycoprotein gp120. In conclusion, X-ray crystallographic analysis of the ternary complex strongly corroborates our theoretically derived model of CD4-Suradista interaction, showing that in both cases essentially the same amino acids are responsible for the stabilization of the complex. Since obtaining single crystals of the putative CD4-Suradista complex, suitable for

X-ray analysis, most likely will still need some time, the model of interaction described here is expected to be helpful for understanding the molecular mechanism implied in the inhibition of CD4-gp120 interaction by Suradista derivatives.

Acknowledgements

We thank Professor P.J. Goodford for kindly providing the program GRID. F.M. wishes to thank Pharmacia & Upjohn, Milan (Italy) for a fellowship. This investigation was supported by Ministero della Sanità, Istituto Superiore di Sanità, 'Progetto Patologia, Clinica e Terapia dell'AIDS', Grant no. 40B.69, 1998.

References

1. Fantini, J. and Sabatier, J.-M., In Fantini, J. and Sabatier, J.-M. (Eds.), HIV Infection in CD4$^-$ Cells, ESCOM, Leiden, The Netherlands, 1996, pp. V–VI.
2. Levy, J.A., Microbiol. Rev., 57 (1993) 183.
3. Miedema, F., Immunodefic. Rev., 3 (1992) 173.
4. Miedema, F., Meynaard, L., Koot, M., Klein, M.R., Roos, M.T.L., Groenink, L., Fouchier, R.A.M., Van't Wout, A.B., Tersmette, M., Schellekens, P.T.A. and Schuitemaker, H., Immunol. Rev., 140 (1994) 35.
5. Bour, S., Geleziunas, R. and Wainberg, M.A., Microbiol. Rev., 59 (1995) 63.
6. Wang, J., Yan, Y., Garrett, T.P.J., Liu, J., Rodgers, D.W., Garlick, R.L., Tarr, G.E., Husain, Y., Reinherz, E.L. and Harrison, S.C., Nature, 348 (1990) 411.
7. Ryu, S.-E., Kwong, P.D., Truneh, A., Porter, T.G., Arthos, J., Rosenberg, M., Dai, X., Xuong, N., Axel, R., Sweet, R. and Hendrickson, W., Nature, 348 (1990) 419.
8. Ramurthy, S., Lee, M.S., Nakanishi, H., Shen, R. and Kahn, M., Biol. Med. Chem., 9 (1994) 1007.
9. Jarvest, R.L., Breen, A.L., Edge, C.M., Chaikin, M.A., Jennings, L.J., Alemseged, T., Sweet, R.W. and Hertzberg, R.P., Biol. Med. Chem. Lett., 3 (1993) 2851.
10. Broder, C.C. and Berger, E.A., J. Virol., 67 (1993) 913.
11. Freed, E.O., Myers, D.J. and Risser, R., J. Virol., 65 (1991) 190.
12. De Rossi, A., Pasti, M., Mamano, F., Panozzo, M., Dettin, M., Di Bello, C. and Chieco-Bianchi, L., Virology, 184 (1991) 187.
13. Nehete, P.M., Arlinghaus, R.H. and Sastry, K.J., J. Virol., 67 (1993) 6841.
14. Mongelli, N., Biasoli, G., Paio, A., Grandi, M. and Ciomei, M. (1991) Eur. Patent no. 91902204.6.
15. Mongelli, N., Crugnola, A., Lombardi Borgia, A., Ciomei, M., Albanese, C. and Sola, F. (1997) U.K. Patent no. 9713732.
16. Biasoli, G., Botta, M., Ciomei, M., Corelli, F., Grandi, M., Manetti, F., Mongelli, N. and Paio, A., Med. Chem. Res., 4 (1993) 202.
17. Manetti, F., Cappello, V., Botta, M., Corelli, F., Mongelli, N., Biasoli, G., Lombardi Borgia, A. and Ciomei, M., Bioorg. Med. Chem., 6 (1998) 947.
18. Clanton, D.J., Buckheit, R.W., Terpening, S.J., Kiser, R., Mongelli, N., Borgia, A.M., Schultz, R., Narayanan, V., Bader, J.P. and Rice, W.G., Antiviral Res., 27 (1995) 335.
19. Mohan, P., Wong, M.F., Verma, S., Huang, P.P., Wickramasinghe, A. and Baba, M., J. Med. Chem., 36 (1993) 1996.
20. Leydet, A., Moullet, C., Roque, J.P., Witvrouw, M., Pannecouque, C., Andrei, G., Snoeck, R., Neyts, J., Schols, D. and De Clercq, E., J. Med. Chem., 41 (1998) 4927.
21. Lederman, S., Bergmann, J.E., Cleary, A.M., Yellin, M.J., Fusco, P.J. and Chess, L., AIDS Res. Human Retroviruses, 8 (1992) 1599.
22. Rusconi, S., Moonis, M., Merril, D.P., Pallai, P.V., Neidhardt, E.A., Singh, S.K., Willis, K.J., Osburne, M.S., Profy, A.T., Jenson, J.C. and Hirsch, M.S., Antimicrob. Agents Chemother., 40 (1996) 234.
23. Patch, R.J., Roberts, J.C., Gao, H., Shi, Z., Gopalsamy, A., Kongsjahju, A., Daniels, K., Kowalczyk, P., van Schravendijk, M.-R., Gordon, K.A. and Pallai, P., Bioorg. Med. Chem. Lett., 24 (1996) 2983.
24. Cushman, M., Insaf, S., Ruell, J.A., Schaeffer, A. and Rice, W., Bioorg. Med. Chem. Lett., 8 (1998) 833.
25. Cushman, M., Golebiewski, W.M., McMahan, J.B., Buckheit, R.W., Clanton, D.J., Weislow, O.S., Haugwitz, R.D., Bader, J.P., Graham, L. and Rice, W.G., J. Med. Chem., 37 (1994) 3040.
26. Program InsightII, distributed by MSI, San Diego, CA.
27. MacroModel and BatchMin, Version 4.5, Columbia University, New York, NY, 1995.
28. Mohamadi, F., Richards, N.G.J., Guida, W.C., Liskamp, R., Caufield, C., Chang, G., Hendrickson, T. and Still, W.C., J. Comput.-Aided Mol. Design, 4 (1990) 440.
29. Guntertofte, K., Liljefors, T., Norrby, P.O. and Pettersson, I., J. Comput. Chem., 17 (1996) 429.
30. Merz, K.M., Murcko, M.A. and Kollman, P.A., J. Am. Chem. Soc., 113 (1991) 4484.
31. Leach, A.R. and Kuntz, I.D., J. Comput. Chem., 13 (1992) 730.
32. Goodford, P.J., J. Med. Chem., 28 (1985) 849.
33. Boobbyer, D.N.A., Goodford, P.J., McWhinnie, P.M. and Wade, R., J. Med. Chem., 32 (1989) 1083.
34. Botta, M., Cernia, E., Corelli, F., Manetti, F. and Soro, S., Biochim. Biophys. Acta, 1296 (1996) 121.
35. Botta, M., Cernia, E., Corelli, F., Manetti, F. and Soro, S., Biochim. Biophys. Acta, 1337 (1997) 302.
36. Guida, W.C., Bohacek, R.S. and Erion, M.D., J. Comput. Chem., 13 (1992) 214.
37. Cushman, M., Insaf, S., Paul, G., Ruell, J.A., De Clercq, E., Schols, D., Pannecouque, C., Witvrouw, M., Schaeffer, C.A., Turpin, J.A., Williamson, K. and Rice, W.G., J. Med. Chem., 42 (1999) 1767.
38. Kwong, P.D., Wyatt, R., Robinson, J., Sweet, R.W., Sodroski, J. and Hendrickson, A., Nature, 393 (1998) 648.
39. Holloway, M.K., In Kubinyi, H., Folkers, G. and Martin, Y.C. (Eds.), 3D QSAR in Drug Design, Kluwer/Escom, Dordrecht, the Netherlands, 1998, pp. 63–84.